

THE ANALYSIS OF A JET STRUCTURE INSIDE A REVERSE CHAMBER

by

Robert KLOSOWIAK*, Jaroslaw BARTOSZEWICZ, and Rafal URBANIAK

Chair of Thermal Engineering, Poznan University of Technology, Poznan, Poland

Original scientific paper
<https://doi.org/10.2298/TSC19S4357K>

The paper presents experimental results for an axisymmetrical jet flow impinging with outflow through a reverse chamber. The test results include the average distributions and fluctuations of pressures on the impinged wall and the side wall of the chamber. The presented results cover further the mean velocities and the velocity fluctuations in the reverse chamber in relation to two velocity components: axial and radial. The purpose of the paper is to indicate the differences between different flow situations: the axisymmetrical free jet, the impinging jet hitting a flat surface, and a flow geometrically alike, however, restricted in outflow through a reverse annular chamber.

Keywords: reverse chamber, circulating jet, axisymmetrical jet, impinging jet

Introduction

Many papers are published in the world's literature every year on free jets and impinging jets. This is the consequence of extremely high demand for experimental test results and numerical simulations covering the technical cases of the occurrence of such flows. One issue with the use of them arises when the free jet test results are attempted to be used for the description of the processes going on inside thermal-flow machines. The free flows encounter obstacles in such machines and they move along the restricting surfaces. The purpose of this paper is, in addition to the presentation of results describing the velocity and pressure distributions in the reverse chambers, to point out the differences between such classes of flows. The investigations on free and impinging jets have their beginnings in the 1960s when papers describing the phenomena occurring in planar jets, Bradbury [1], and round impinging jets, Gardon and Akfirat [2], were presented. In both cases, the papers were devoted to the description of mass, momentum, and energy in the jet and between the jet and solid surface. The tools applied for such analysis in those years were based on anemometric techniques, Heskestad [3]. The 1970s saw a significant growth of publications on free jets and contributed to the precise description of the phenomena occurring in free and impinging jets. Such papers as Crow and Champagne [4], Wygnanski and Peterson [5], Gutmark and Wygnanski [6] provided the understanding of the structure of such jets. Further, authors performed experimental study to analyse the fluid mechanic processes and their correlations within the jets, Winant and Browand [7], Brown and Roshko [8], Cohen and Wygnanski [9], and Popiel and Bogusławski [10]. The late 1980s brought a dynamic growth of papers related to the numerical

* Corresponding author, e-mail: robert.klosowiak@put.poznan.pl

modeling of free jets and the turbulence description within the jets, in particular, *e. g.* Launder and Rodi [11]. Ever since then and until the present, every year we see more and more works on free jets and the descriptions of their interaction with solids. The issues the authors try to solve, however, are much more complex than those occurring in the past. Relevant from the point of view of free and restricted jets are the following test results: evolution of free jet flowing out of ventilation and being transformed into a wall jet, Cho *et al.* [12], the natural convection effect on the heat exchange processes near the impinged surface Koseoglu and Baskaya [13], the effect of large temperature gradients on the transport processes on the impinged surface, Shi *et al.* [14] or energy transformation in turbulent flow inside reversing chamber, Bartoszewicz *et al.* [15]. A separate group of papers are those describing the transport processes between free jets and rotating surfaces, Sara *et al.* [16], descriptions of the correlations between the stresses on the impinged walls, appearing as a result of free jet in-flow and helpful with corrosion reduction, Demoz and Dabros [17], descriptions of free jet deformation due to the action of transverse jets in the outlet nozzle, Tamburello and Amitay [18], transverse flame deformation under external influence, Hourri *et al.* [19], or finally the tests on velocity distribution in the fluidal deposit the gas jet flows through, Ounnar *et al.* [20]. The papers referred here indicate the wide use of free and impinging jets in technology [7, 18, 21, 22]. Most of the authors indicate that the location of the phenomenon is in thermal-flow machines, Slefarski *et al.* [23], and this type of flows is within the restricted flow class. The papers mentioned brought information on the structure and form of the free jet.

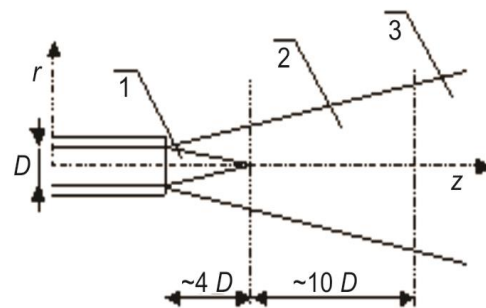


Figure 1. The schematics of axis-symmetrical free jet; 1 – potential core, 2 – region of strong gradient, and 3 – region of uniform turbulence

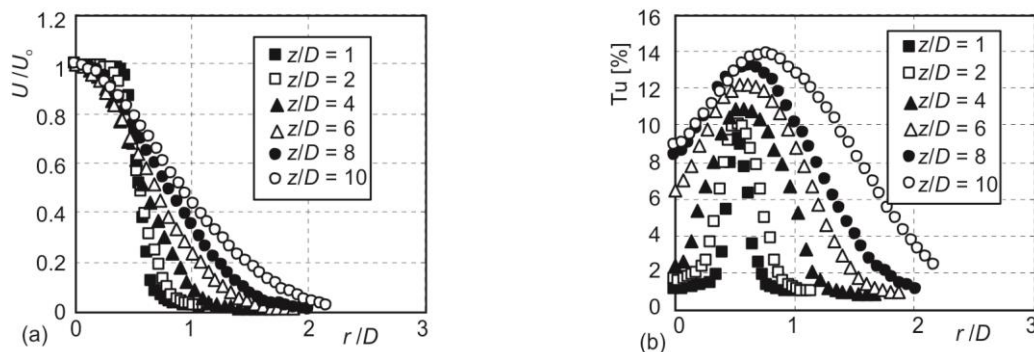


Figure 2. The radial distributions of centerline normalized axial velocity (a) and turbulence intensity (b) for varying distance from the outlet of the nozzle [24]

Figure 1 shows the schematics of a free jet, and figs. 2 and 3 show the standardized velocity distributions in the function of distance from the outlet nozzle, radial turbulence grade profiles and the axial distribution of standardized axial velocity component and its fluctuations.

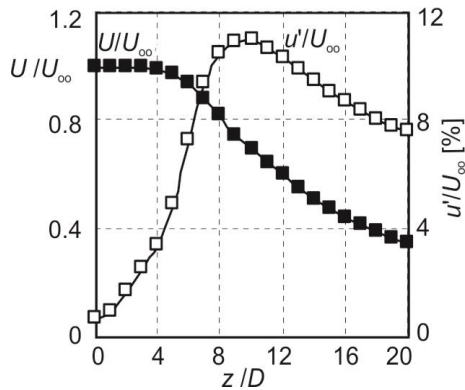


Figure 3. The axial distribution of centerline normalized axial velocity and its fluctuations [24]

Geometric model and test methods

The object of the tests is the axisymmetrical reverse chamber shown in fig. 4(a). The main flow direction changes twice in the reverse chambers. The jets flowing out of the internal pipe, in its initial behavior, is of free jet nature, and then it impinges the flat surface of the chamber bottom, where the flow direction for the first time changes by 90°. Within the inflowing jet's axis, at the so-called stagnation point, the maximum pressure occurs. Such flow can be given a simplified definition of the impinging jet. Upon change of direction, the wall jet heads towards the radial direction. Before it reaches the flow wall, however, it separates from the impinged wall and thus a second stagnation point is located on the side wall near the reverse

chamber corner. The jet changes its flow direction by the 90° angle again. From this point, the counter-flow in relation to the basic jet flowing out of the internal pipe, heads towards the reverse chamber outlet. As the distance from the outlet wall increases, the wall jet may tear apart from the flow wall in a location depending on the jet's kinetic energy. The test chamber reflecting the nature of such flow is built of a steel sharp-edged pipe of internal diameter $D = 0.04$ m and 0.005 m thickness. The chamber casing was made of plexiglass of internal diameter $R = 0.198$ m and length 0.7 m. A photo of the test chamber is presented in fig. 4(b) with pressure measuring points on the impinged wall and on the side wall. The points are distributed unevenly. The distribution of the measuring points was based on the results of numerical calculations with the use of the Phoenix code, Rosten and Spalding [25]. A sliding ring with ten radial supports bracing the chamber is visible on the right side, enabling its sliding along the internal pipe and achievement of coaxiality of the chamber in relation to the internal pipe. It enables the change of the distance between the internal pipe outlet and the impinged surface.

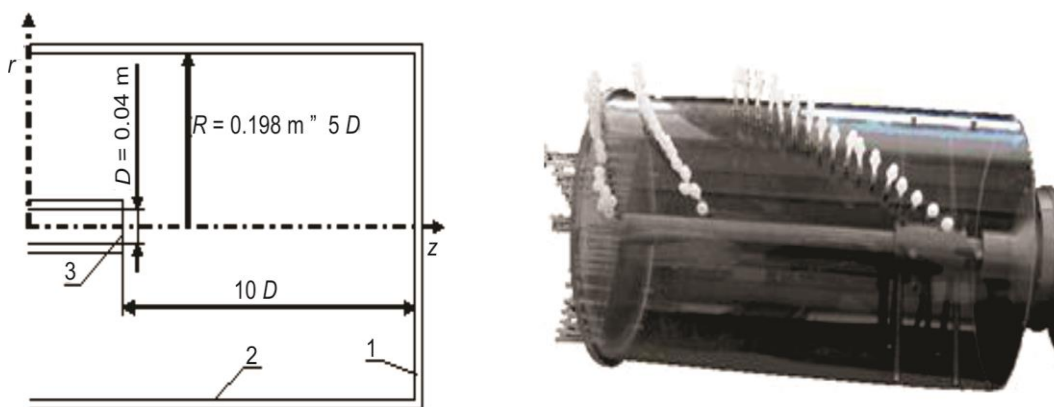


Figure 4. The schematics of reverse chamber; 1 – impinged wall, 2 – side wall, 3 – outlet of pipe (a) and photo of the reverse chamber with pressure measuring points (b)

Boundary conditions

The measurements were made on an axisymmetrical non-swirled and unstimulated jet flowing out through the sharp-edged circular channel of 0.04 m diameter to the reverse chamber of 0.1 m diameter. The geometric conditions corresponded to the pipe outlet from the impinged surface: $z/D = 10$. The boundary conditions in which the measurements were made included air outflow velocity changes from the internal pipe of the reverse chamber. The measurements were made for three velocities: 10, 30, and 50 m/s, which correspond to Reynolds numbers of 26000, 78000, and 130000, respectively. The air temperature was maintained at 20 °C. The tests included average values in time for pressures, axial velocity component and radial velocity component, and the fluctuations of the radial and axial component, Heskestad [3].

Results

All the results of the experimental tests will be presented in the form of figures normalized by the maximum value of pressure or axial velocity component. This will allow the assessment of qualitative differences in distributions that will form explicit information on the possible changes of phenomena occurring at the flow with various velocities. The maximum axial velocity value falls within the outflow jet distance from the pipe outlet and along the potential core section. The data will be presented in the function of normalized positions as radial and axial distributions. The positions were normalized by the internal pipe diameter, D . The normalization of the position co-ordinates allows an indication of differences in the courses being the consequence of changes in the phenomena accompanying the flow.

Figures 5 and 6 are present the static pressure measurement results and their fluctuations on the surfaces of the impinged wall and the side wall surfaces. The static pressure difference measurements were made based on 94 points located on the impinged surface and the outflow surface. The normalized radial distribution of the static pressure for various velocities does not show any significant differences. The zone of increased pressure reaches up to $r/D = 1.8$ in the radial direction, while it is restricted in the unconfined impinging jet at a distance of about $r/D = 1$. This is the effect of main flow direction change near the side wall. For the jet impinging at the wall, appears region with pressures below ambient pressure, and this the first change of the main jet direction. This effect cannot be observed in the case with free jets impinging flat surfaces. This difference shows explicitly the difference in the nature of energy conversion between kinetic energy and pressure.

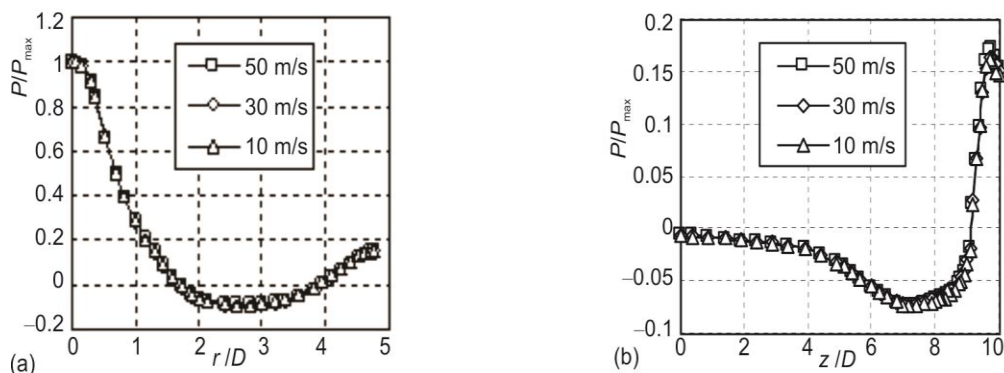


Figure 5. Distributions of pressure on impinged (a) and side walls (b)

Figure 5(b) shows the growth of static pressures in the corner before it drops. The defined pressure value is zero at the distance $z/D = 9$ to the pipe outlet and the minimum is located at a distance of about $z/D = 7-8$. The differences in distributions obtained for the different velocities are scarcely visible. In case of static pressure fluctuation changes are shown in fig. 6. The distributions obtained for various velocities, however, show significant variations. The highest values are obtained for the lowest inflow velocity, *i. e.* for the lowest pressure value in the stagnation point. This means that the pressure fluctuation level is not a direct function of pressure in the stagnation point, but it is the consequence of energy and momentum transport from velocity fluctuation to pressure fluctuation during turbulent motion.

The distributions of the pressure fluctuations correspond to the results obtained for free impinging jets with local maximum at the distance $r/D = 0.5$, and gradual reduction to zero or the surrounding level. In case of the reverse chamber another growth of pressure fluctuation was recorded on the impinged wall, corresponding to the position of the side wall in relation to the second stagnation point. As the chamber is axisymmetrical and the flow has in the mean a radial direction, it should be considered that we have a stagnation area located on the outflow surface. The distribution of pressure fluctuation on the outflow surface in all the three cases has a distribution with a local maximum at a position $z/D = 9.6$ from the pipe outlet and a local minimum at a position $z/D = 8$. The pressure fluctuation level grows from this point to the location $z/D = 6$ and then constantly drops in the direction of outlet from the reverse chamber. At the position $z/D = 6$ one could expect the existence of the jet separation point from the side wall responsible for this local fluctuation increase. However, it is impossible to indicate the separation point accurately basing on the pressure fluctuation measurements alone, because their maximum does not coincide directly with the stagnation point.

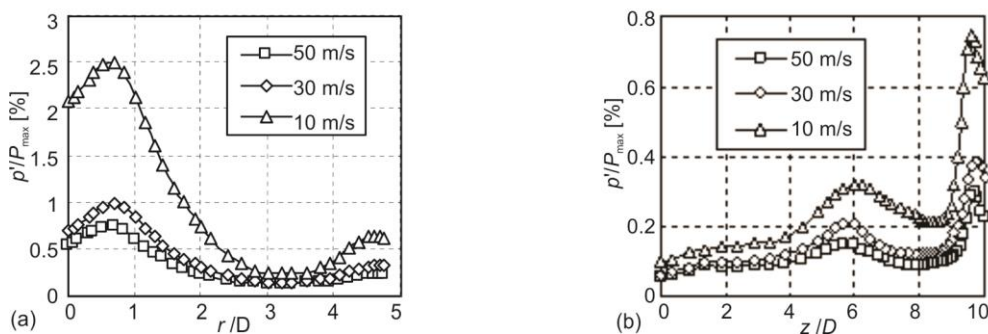


Figure 6. Distributions of pressure fluctuations on impinged (a) and side walls (b)

Figure 7 presents the normalized distributions of the axial velocity component. This figure shows the radial distributions for the three different main jet flow velocities. The normalization is chosen to allow a direct comparison to the distributions for a free jet as given in fig. 2(a). As for the impinging jet, the velocity redistributes in the chamber in a faster manner. The process supplements information on pressure changes on the wall being the effect of faster change of main motion directions and transformation into a counterflow jet. In the reverse chamber situation, the significant velocity drop at the axis is observed at distances of about $z/D = 6-7$ from the pipe outlet. In the central part of the jet, like in the free jets, no effects of the velocity magnitude on the normalized distributions were recorded. A different situation occurs in the boundary area of the side wall. Between the distances $z/D = 7-9$ the radial veloc-

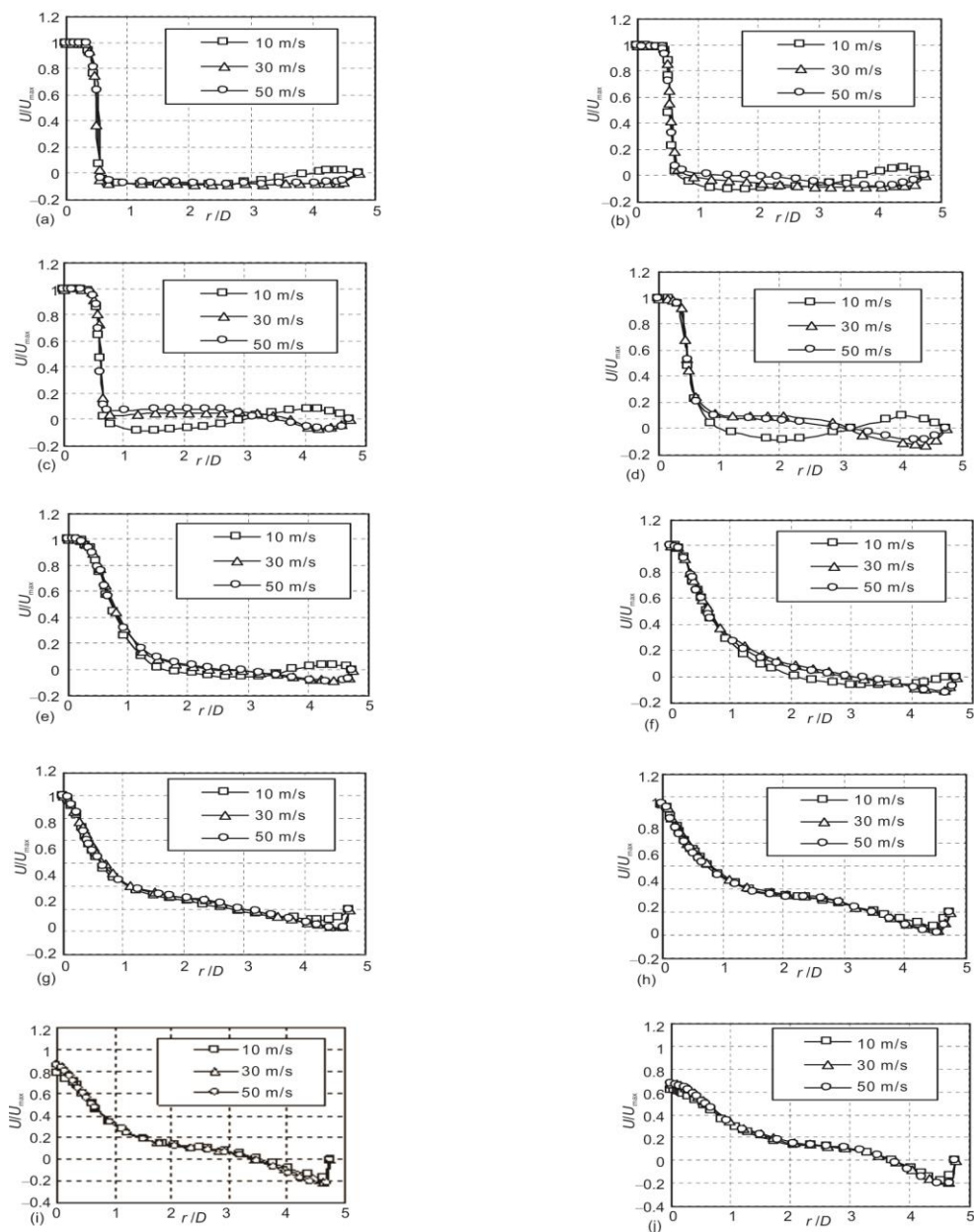


Figure 7. The radial distribution of axial component of velocity for different mean velocities; (a) $z/D = 0$, (b) $z/D = 1$, (c) $z/D = 2$, (d) $z/D = 3$, (e) $z/D = 4$, (f) $z/D = 5$, (g) $z/D = 6$, (h) $z/D = 7$, (i) $z/D = 8$, and (j) $z/D = 9$

ity profiles are alike and the jets behave in a similar way. The distance $z/D = 6$ is the starting point where the difference in the shapes and nature of the flow becomes visible for velocity 10 m/s. With the distance $z/D = 5$ the jet separates from the side wall. The counterflow jet is directed through the central part of the chamber to the outlet whereas the jet with direction

corresponding to that of outflow from the pipe is given by the positive values of velocities in fig. 7(a)-7(e). In case of mean velocities of 30 and 50 m/s the jets behave as wall jets, heading towards the outlet and gradually expanding in the direction of the side wall relative to the jet axis. We observe relocation of the crossing point through the X-axis profiles from $r/D = 3$ in fig. 7(d) to $r/D = 2$ in fig. 7(b). At $z/D = 0$ the jet fills the whole cross-section of the reverse chamber between the internal pipe and the side wall. For those two velocities in the central part of the reverse chamber, a swirl with the center located in the distance $r/D = 2$ is formed, which is represented by local maxima in figs. 7(d) and 7(e). In figs. 7(i) and 7(j) a slight difference in the distribution for the 10 m/s case is noticeable, which should be connected with the different nature of the flow near the side wall determining the structure in the stagnation area.

Tests on the restricted jet, in this case by the side wall situated axisymmetrically, causes the occurrence of phenomena that do not occur in axisymmetrical free, non-stimulated jets in the flow. The most important element out of them is the appearance of the second stagnation point on the side wall. The course of the radial component from the wall starts with zero and, through negative values, the local minimum passes zero another time until the local maximum has been reached. The static pressure level changes from a value above zero on the impinging wall to the maximum in the point where the radial component assumes the zero value. Zeroing of the radial component is the necessary, however insufficient, condition to reach the stagnation point. The axial component also must have a zero value in this point, which is shown in the drawing. The appearance of the positive axial component means that a swirl rotating towards the impinging wall is located in this area. The main jet heads towards the outlet of the reverse chamber, which is determined by the negative values of the axial velocity component. The negative values of the radial component mean that the jet moves away from the wall to the separation point.

The experimental tests were carried out for the changing air outflow from the internal pipe. The measurements made proved the variability of average distributions and fluctuations in the jet. The lowest effect is observed around the outflow axis where the phenomena are determined by the outflow conditions, *i. e.*, they are similar to free jets. The differences are also slight around the chamber's axis. The first differences were detected in the under pressure region on the impinged wall and around the second stagnation point. In this case, pressure growth in the second stagnation point along the velocity increase has been observed. The effect is related to the high energy value of the jet and the same delay in the second change of the main flow direction. The largest differences are observed in the counterflow jet. In the upper part of the outflow direction and in the lower part there are points of swirling areas appearance. Regardless of the velocity value, the swirl near the second stagnation point is present in the outlet cross-section from the pipe. The swirl area decreases with velocity growth. The location of another swirl depends on velocity growth. For velocity of 10 m/s the swirl area is located in the boundary zone of the side wall, while for higher velocities in the observed part of the reverse chamber, no swirl appeared therein. Such effect is achieved upon reaching velocity high enough that the jet, after changing its main direction for the second time, moves along the side wall. In such situation, an alternative swirl area appears between the jet flowing out of the pipe and the counterflow jet.

Summary

The presented experimental test results are the first ones concerning the research on restricted jets of apparently similar nature to free jets. The measuring results indicated significant differences between the free flows: the free and impinging jet; the restricted flows; the

flow through the reverse chamber. The restriction by the side wall introduces its effect on the jet structure in the outflow axis zone and the impinging wall.

All the previous observations confirm the fact of different nature of the jet flow in the reverse chamber as compared to that of free jets. Therefore, it is certain that the use of results of investigations on free and impinging jets in the description of changes in chamber reverses flow taking place inside the thermal-flow machines are not proper.

Nomenclature

D	— diameter of pipe inside reverse chamber, [m]	U_{\max}	— maximal value of axial component of velocity in chamber, [ms^{-1}]
k	— kinetic energy of turbulence, [Jkg^{-1}]	u'	— fluctuation of axial component of velocity, [ms^{-1}]
P	— static pressure, [Pa]	V	— radial component of velocity, [ms^{-1}]
P_{\max}	— static pressure in stagnation point, [Pa]	v'	— fluctuation of radial component of velocity, [ms^{-1}]
p'	— fluctuation of static pressure, [Pa]	z	— axial co-ordinate, [m]
R	— radius of reverse chamber, [m]	<i>Greek symbols</i>	
R	— radial co-ordinate, [m]	τ	— shear stresses, [Pa]
$r1$	— initial radius of the nozzle, [m]	τ_{\max}	— maximal value of shear stresses in profile, [Pa]
$r2$	— final radius of the nozzle, [m]		
Tu	— turbulence intensity, [%]		
U	— axial component of velocity, [ms^{-1}]		
U_o	— axial component of velocity in axis of impinging jet, [ms^{-1}]		

References

- [1] Bradbury, L. J. S., The Structure of a Self-Preserving Turbulent Planar Jet, *Journal of Fluid Mechanics*, 23 (1965), 1, pp. 31-64
- [2] Gardon, R., Akfirat, J. C., The Role of Turbulence in Determining the Heat Transfer Characteristics of Impinging Jets, *International Journal of Heat and Mass Transfer*, 8 (1965), 10, pp. 1261-1272
- [3] Heskestad, G., Hot-Wire Measurements in a Plane Turbulent Jet, *Trans. ASME Journal of Applied Mechanics*, 32 (1965), 4, pp. 721-734
- [4] Crow, S. C., Champagne, F. M., Orderly Structure in Jet Turbulence, *Journal of Fluid Mechanics*, 48 (1971), 3, pp. 547-591
- [5] Wygnanski, I., Peterson, R. A., Coherent Motion in Excited Free Shear Flows, *AIAA Journal*, 25 (1987), 2, pp. 201-213
- [6] Gutmark, E., Wygnanski, I., The Planar Turbulent Jet, *Journal of Fluid Mechanics*, 73 (1976), 3, pp. 465-495
- [7] Winant, C. D., Browand, F. K., Vortex Pairing the Mechanism of Turbulent Mixing Layer Growth at Moderate Reynolds Number, *Journal of Fluid Mechanics*, 63 (1974), 2, pp. 237-255
- [8] Brown, F. K., Roshko, A., On the Density Effects and Large Structure in Turbulent Mixing Layers, *Journal of Fluid Mechanics*, 64 (1974), 4, pp. 775-816
- [9] Cohen, J., Wygnanski, I., The Evolution of Instabilities in the Axisymmetric Jet. Part 1. The Linear Growth of Disturbances Near the Nozzle, *Journal of Fluid Mechanics*, 176 (1987), Mar., pp. 191-219
- [10] Popiel, Cz. O., Boguslawski, L., Mass or Heat Transfer in Impinging Single, Round Jets Emitted by a Bell-Shaped Nozzle and Sharp-Ended Orifice, *Proceedings, 8th International Heat Transfer Conference*, San Francisco, Cal., USA, Vol. 3, pp. 1187-1192, 1986
- [11] Launder, B. E, Rodi, W., The Turbulent Wall Jet - Measurement and Modeling, *Annual Review of Fluid Mechanics*, 15 (1983), Jan., pp. 429-459
- [12] Cho, Y., *et al.*, Theoretical and Experimental Investigation of Wall Confluent Jets Ventilation and Comparison with Wall Displacement Ventilation, *Building and Env.*, 43 (2008), 6, pp. 1091-1100
- [13] Koseoglu, M. F., Baskaya, S., Experimental and Numerical Investigation of Natural Convection Effects on Confined Impinging Jet Heat Transfer, *International Journal of Heat and Mass Transfer*, 52 (2009), 5-6, pp. 1326-1336
- [14] Shi, Y., *et al.*, Effect of Large Temperature Difference on Impingement Heat Transfer Under a Round Turbulent Jet, *Int. Comm. Heat Mass Transfer*, 31 (2004), 2, pp. 251-260

- [15] Bartoszewicz, J., *et al.*, The Analysis of the Flow Structure in a Jet At Variable Geometry of the Reverse Chamber, *International Journal of Heat and Mass Transfer*, 55 (2012), 11-12, pp. 3239-3245
- [16] Sara, O. N., *et al.*, Electrochemical Mass Transfer Between an Impinging Jet and a Rotating Disk in a Confined System, *International Communications in Heat and Mass Transfer*, 35 (2008), 3, pp. 289-298
- [17] Demoz, A., Dabros, T., Relationship Between Shear Stress on the Walls of a Pipe and an Impinging Jet, *Corrosion Science*, 50 (2008), 1, pp. 3241-3246
- [18] Tamburello, D. A., Amitay, M., Active Control of a Free Jet Using a Synthetic Jet, *International Journal of Heat and Fluid Flow*, 29 (2008), 4, pp. 967-984
- [19] Hourri, A., *et al.*, Surface Effects on Flammable Extent of Hydrogen and Methane Jets, *International Journal of Hydrogen Energy*, 34 (2009), 3, pp. 1569-1577
- [20] Ounnar, A., *et al.*, Hydrodynamic Behavior of Upflowing Jet in Fluidized Bed: Velocity Profiles of Sand Particles, *Chemical Engineering and Processing*, 48 (2009), 2, pp. 617-622
- [21] Szewczyk, D., *et al.*, Analysis of the Combustion Process of Syngas Fuels Containing High Hydrocarbons and Nitrogen Compounds in Zonal Volumetric Combustion Technology, *Energy*, 121 (2017), Feb., pp. 716-725
- [22] Urbaniak, R., *et al.*, Main Causes of NO_x Emissions by Low-Power Boilers, *Polish Journal of Environmental Studies*, 24 (2015), 5, pp. 2223-2230
- [23] Slefarski, R., *et al.*, Experimental Investigation on Syngas Reburning Process in a Gaseous Fuel Firing Semi-Industrial Combustion Chamber, *Fuel*, 217 (2018), 1, pp. 490-498
- [24] Klosowiak, R., *et al.*, Energy Transformation in Turbulent Flow Inside Reversing Chamber, *Proceedings*, 23rd International Conference Engineering Mechanics, Svratka, Czech Republic, pp. 466-469, 2017
- [25] Rosten, H. I., Spalding, D. B., The Phoenix Beginners Guides, CHAM report, No TR100, CHAM Limited, Wimbledon, UK